Catalysis Letters Vol. 107, Nos. 1–2, February 2006 (© 2006)
DOI: 10.1007/s10562-005-9730-1

Effect of vanadium promotion on activated carbon-supported cobalt catalysts in Fischer–Tropsch synthesis

Tao Wang[a,c], Yunjie Ding[a,b,*], Jianmin Xiong[a], Li Yan[a,c], Hejun Zhu[a], Yuan Lu[a], and Liwu Lin[a,b]

[a]*Natural Gas Utilization and Applied Catalysis Laboratory, Dalian, China*
[b]*State Key Laboratory of catalysis, Dalian Institute of Chemical Physics, Chinese Academy of Sciences, Dalian 116023, China*
[c]*Graduate School of Chinese Academy of Science, Beijing, China*

Received 8 October 2005; accepted 18 October 2005

The effect of vanadium promotion on activated carbon (AC)-supported cobalt catalysts in Fischer–Tropsch synthesis has been studied by means of XRD, TPR, CO-TPD, H_2-TPSR of chemisorbed CO and F-T reaction. It was found that the CO conversion could be significantly increased from 38.9 to 87.4% when 4 wt.% V was added into Co/AC catalyst. Small amount of vanadium promoter could improve the selectivity toward C_{10}–C_{20} fraction and suppress the formation of light hydrocarbon. The results of CO-TPD and H_2-TPSR of adsorbed CO showed that the addition of vanadium increased the concentration of surface-active carbon species by enhancing CO dissociation and further improved the selectivity of long chain hydrocarbons. However, excess of vanadium increased methane selectivity and decreased C_5^+ selectivity.

KEY WORDS: AC-supported Co catalyst; Fischer–Tropsch synthesis; vanadium promotion.

1. Introduction

The Fischer–Tropsch synthesis (FTS) is a promising option for converting coal or natural gas-derived syngas (CO/H_2 mixture) to the high quality clean liquid fuels and high value chemicals. Cobalt catalysts are the preferred catalysts for the Fischer–Tropsch synthesis due to their high activity and high selectivity for linear hydrocarbons, low water-gas shift activity and lower price compared to noble metal [1,2]. In the Fischer–Tropsch synthesis, since the active phase is metallic cobalt, having the cobalt well reduced and dispersed is required to have high activity. Silica and alumina are commonly used as supports for cobalt-based catalyst, but activated carbon is considered to be more inert than silica and alumina [3]. The inert of the surface facilitates the reduction of the metal precursor to the zero-valence state. On the other hand, owing to their specific features, such as high surface area, porosity and surface chemistry, activated carbon can affect the activity and selectivity of the catalyst [4].

Much attention has been paid to the modification of the catalytic activity and selectivity for the Fischer–Tropsch synthesis by means of promoters in the last few years. A number of studies have demonstrated that addition of modifiers (e.g. Pt [5], Ru [6,7], Re [8], La [9,10], Zr [11,12], Th [13]) to cobalt catalysts can increase reducibility, activity and selectivity to long chain hydrocarbon. It is mentioned in the literature that V-promoted Rh catalysts could significantly improve both the activity and selectivity towards the formation of C_2 oxygenates such as ethanol and acetic acid [14]. Meanwhile, the results of patent suggested that V promotion of Co-based catalyst was efficient for the Fischer–Tropsch synthesis [15]. Guerrero-Ruiz *et al.* [16] have also found that the addition of oxide promoters (MgO, V_2O_5, CeO_2) enhanced specific activity and selectivity on Ru/C, Co/C catalysts in CO hydrogenation.

Our previous work indicated that activated carbon-supported Co catalyst favored the formation of C_{10}–C_{20} hydrocarbon in Fischer–Tropsch Synthesis [17]. Meantime, we have also reported that the addition of ZrO_2 into Co/AC catalyst could increase CO conversion and enhance the selectivity to C_{10}–C_{20} hydrocarbon [17,18]. The purpose of this study was to investigate the influence of V promotion on the catalytic performance of Co/AC catalysts for the CO hydrogenation.

2. Experimental

2.1. Catalyst preparation

Co-based catalysts with different V loadings were prepared by aqueous incipient wetness impregnation. The Co loading was 15 wt.% in all the catalysts. In order to eliminate the mineral impurities, the activated carbon support (obtained from Beijing guanghua, almond carbon) was sieved to 20–40 mesh and washed with distilled water before being used. The specific surface area was characterized to be 862.2 m^2/g with pore volume of 0.34 cm^3/g. At the first step, the activated carbon was impregnated with a solution of $VO(NO_3)_3$,

* To whom correspondence should be addressed.

then it was dried at room temperature and calcined at 623 K for 6 h in a flow of N_2 (40 mL/min). Sequentially, it was further impregnated with $Co(NO_3)_2{\cdot}6H_2O$ solution, then dried at 393 K for 10 h and calcined at 623 K for 6 h in a flowing nitrogen at 40 mL/min.

2.2. XRD measurement

X-ray powder diffraction patterns of samples were recorded on a Philips X Pert PRO diffractometer using Cu kα radiation at 40 kV and 30 mA. The spectra were scanned at a rate of 2.4°/min in the range of $2\theta = 30-75°$.

2.3. Temperature-programmed reduction (TPR)

The TPR analysis was carried out on America Micromeritics Autochem 2910 equipment. About 100 mg of catalyst was placed in a quartz reactor and reduced by a 10% H_2–Ar gas mixture in a flow rate of 50 mL/min. The temperature was elevated from room temperature to 1173 K at a rate of 10 K/min and the hydrogen consumption was recorded with the thermal conductivity detector. The TPR was calibrated using the reduction of Ag_2O powder.

2.4. Temperature programmed desorption (CO-TPD)

Temperature programmed desorption of adsorbed CO was carried out in a flow apparatus of America Micromeritics Autochem 2910. The catalyst sample (ca. 100 mg) was placed in a quartz reactor and reduced by flowing H_2 at 673 K for 1 h, then purged by He at the same temperature for 0.5 h. When it was cooled to room temperature, 5% CO–He was introduced in pulse mode for adsorption. After CO adsorption saturation was achieved, the catalyst was swept with He for 30 min. Finally, the temperature was elevated from room temperature to 1173 K at heating rate of 10 K in a He flow at 20 mL/min. The product ($m/z = 15(CH_4)$, $18(H_2O)$, $28(CO)$ and $44(CO_2)$) was simultaneously detected with a Balsers OmniStar 300.

2.5. Temperature-programmed surface reaction (H_2-TPSR)

Temperature-programmed surface reaction (H_2-TPSR) experiments were conducted on the same apparatus in CO-TPD experiment as described above. A 100 mg sample was reduced in a flow H_2 at 673 K for 1 h, and then purged by a He flow at the same temperature for 0.5 h. CO was adsorbed by flowing a 5% CO–He mixture at ambient temperature for 30 min. Physical adsorbed CO was purged with a He flow for 30 min. Finally, a flow of 20 ml/min 10% H_2-Ar was passed through the catalyst bed when the temperature was ramped at 10 K/min from 300 K to 1173 K. MS signal at $m/z = 15$ (CH_4) was recorded.

2.6. Fischer–Tropsch reaction

The F-T reaction was performed using a high-pressure fixed bed reactor. The samples were *in situ* reduced in a flow of H_2 at 673 K for 16 h before reaction. Then the syngas ($H_2/CO = 2$) was fed into catalyst bed and maintained the reaction conditions of 493 K, 2.5 MPa and GHSV = 500 h^{-1}. The tail gas was on-line analyzed by Varian CP-3800 GC with a Porapak QS column and TCD detector. C_4–C_{26} hydrocarbons in the oil phase of F-T products were off-line analyzed on Varian CP-3800 with SE-54 capillary column and FID detector. In order to determine the possibility of AC methanation under Fischer–Tropsch synthesis conditions, we detected the composition of the products during reduction (reaction temperature was higher than that of F-T reaction) in a H_2 flow. The results obtained show that the methanation of activated carbon carrier under the F-T reaction conditions can be ignored.

3. Results and discussion

3.1. X-ray diffraction

The XRD patterns of the Co/AC and V–Co/AC samples calcined in a N_2 flow at 623 K are shown in figure 1. The diffraction peak at 36.8° corresponds to the Co_3O_4, while the other peaks at 42.4° and 61.5° are assigned to CoO species. Many literatures reported that when cobalt nitrate was impregnated on SiO_2 or Al_2O_3, and followed by calcination at high temperature, Co_3O_4 was found to be the dominant Co species [19]. CoO species in our samples might result from the reduction of partial Co_3O_4 due to some organic groups on the surface of activated carbon acting as a reducing agent.

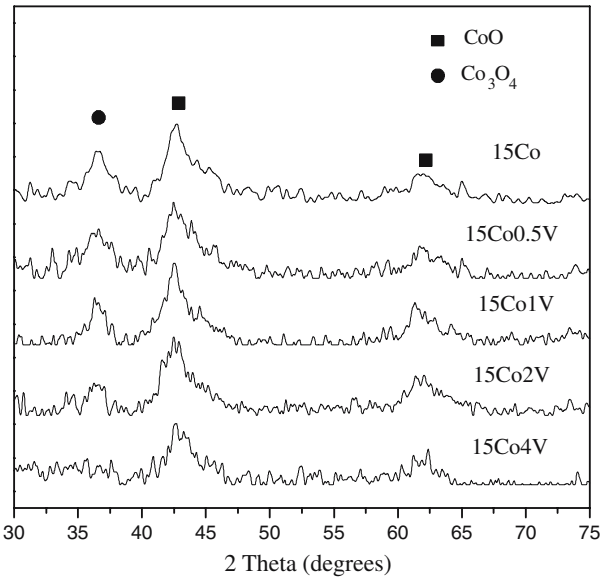

Figure 1. XRD pattern of Co-based catalysts with various V loadings after calcination in a N_2 flow.

However, Khodakov *et al*. [20] reported that the presence of CoO was observed on the Co/SiO_2 catalyst heated under N_2 at 623–673 K. This probably indicates that heating of the Co/AC sample under inert atmosphere results in reduction of the Co_3O_4 and its partial transformation to the CoO species. In the case of V–Co/AC catalyst, it is obvious that the diffraction peak of Co_3O_4 becomes weak. It can also be seen that no diffraction of V_2O_5 or the other vanadium oxides peak is observed, implying V species well disperses on the surface of Co/AC catalysts.

Figure 2 shows XRD patterns of Co/AC samples with different V loadings after F-T reaction. The diffraction peak of the cobalt metal phase was detected at $2\theta = 44.5°$. It is clear that the diffraction peak of Co metal becomes weaker and broader with increase of V loading. The average Co metal particle size calculated from line broadening analysis by the Scherrer equation is shown in table 1. The results show that the average size of cobalt particles of used 15Co/AC is about 17.8 nm, while that of used 15Co4V/AC is 12.5 nm. It is evident from these data that the existence of V on the surface of activated carbon hinders the aggregation of cobalt species even in the presence of water formed during the Fischer–Tropsch reaction.

3.2. Temperature-programmed reduction

The TPR profiles of the vanadium-modified Co/AC catalysts are shown in figure 3. Four reduction peaks are exhibited for all catalysts. The three major peaks are found at 587 K (peak β), 734 K (peak γ) and 848 K (peak δ). The first two maximum hydrogen consumption peaks can be assigned to the two-step reduction of Co_3O_4 to CoO and CoO to Co [21,22]. The broad reduction peak between 630 K and 900 K (maximum at 848 K) is attributed to the methane formation, which is originated from the reduction of the surface functional group on the activated carbon surface by H_2 [16,23]. The weak shoulder peak at 496 K (peak α) due to decomposition of residual cobalt nitrate on the catalyst is also observed. The magnitude of this shoulder peak has been shown to depend on calcinations condition [24].

Table 1
Average size of metallic cobalt crystallite of catalysts after reaction using Scherrer equation

Catalyst	*d* (Co) nm
15Co	17.8
15Co0.5V	14.2
15Co1V	13.9
15Co2V	13.4
15Co4V	12.5

The quantitative analysis results of the degree of reduction on V-promoted Co/AC catalysts might be calculated from the TPR profiles (see table 2). It is well known that the reduction of Co_3O_4 to Co passes through CoO, therefore, the two-step reduction proceeds as follows: $Co_3O_4 + H_2 \rightarrow 3CoO + H_2O$; $3CoO + 3H_2 \rightarrow 3Co + 3H_2O$. The stoichiometric H_2 consumption ratio associated with the two reduction steps is 0.33:1. However, since reduction of Co_3O_4 is kinetically limited [25], the β broad peak will contain a small contribution from reduction of CoO to metallic Co. This is likely the reason why the calculated value of Co/AC catalyst in table 2 is slightly higher than 0.33. The

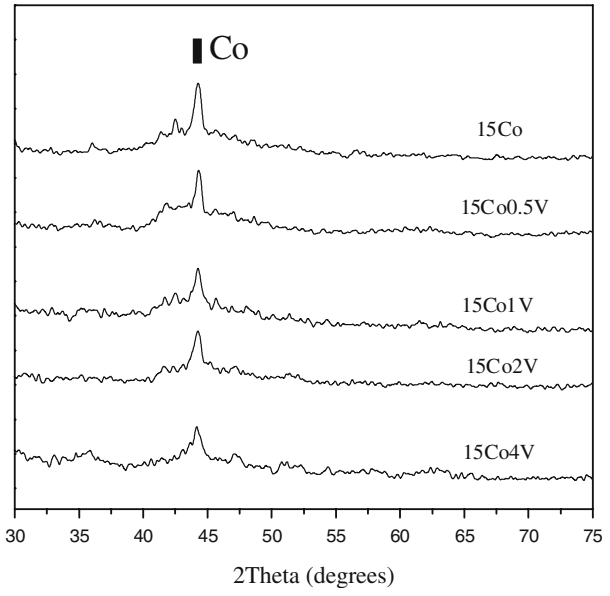

Figure 2. XRD patterns of Co-based catalysts with various V loadings after reaction.

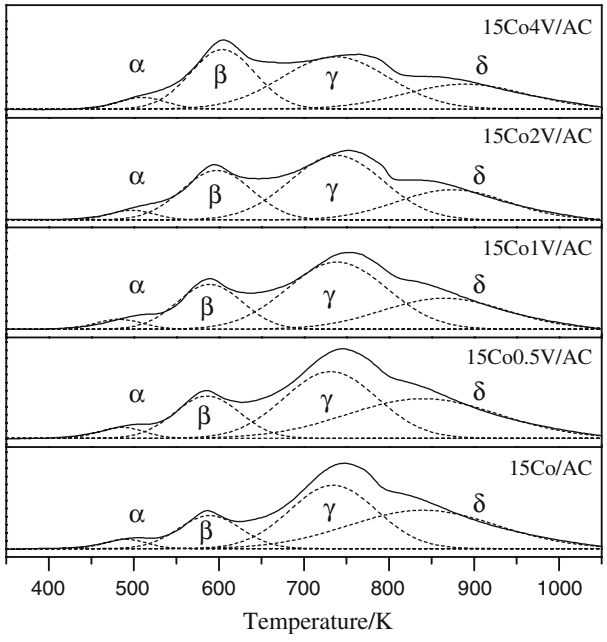

Figure 3. TPR profiles for Co/AC and V–Co/AC catalysts before reaction.

Table 2
The consumption of H_2 during the TPR and the reducibility of Co-based catalysts

Catalyst	H_2 consumption (μmol)					β/γ	Reducibility (%) (470–930 K)
	α	β	γ	δ	Total		
15Co	11.6	61.3	163.2	169.1	405.2	0.38	75.4
15Co0.5V	14.7	81.9	184.1	177.9	458.6	0.44	85.2
15Co1V	9.50	102.4	177.4	145.8	435.1	0.58	93.9
15Co2V	4.10	113.2	167.7	84.9	369.9	0.68	94.5
15Co4V	16.2	117.1	164.8	89.7	387.8	0.71	95.1

hydrogen consumption ratio for the peak β to the peak γ of the V modified Co/AC catalysts between 470 K and 700 K is obviously higher than that of Co/AC catalyst, which indicates reduction of more cobalt oxide to metallic Co. It is clear that modification of Co/AC catalyst by vanadium favors to increase reducibility of cobalt oxide.

3.3. Temperature programmed desorption (CO-TPD)

CO-TPD is a powerful tool to explain by assuming a reinforcement of the CO-metal bond with a subsequent C–O bond weakening, it also provides information about adsorbed CO dissociation. Figure 4 displays the TPD spectra of adsorbed CO on Co/AC catalyst. Three desorption peaks of CO appear at 392, 811 and 912 K, respectively, in CO-TPD profile of the Co/AC catalyst. The small peak at low temperature (392 K) is due to desorption of a weakly adsorbed CO while the middle one at 811 K would arise from a strongly adsorbed CO [26,27]. The third big peak at 912 K might be assigned to the decomposition of superficial oxygen complexes formed during activated carbon preparation or subsequent oxidation [28].

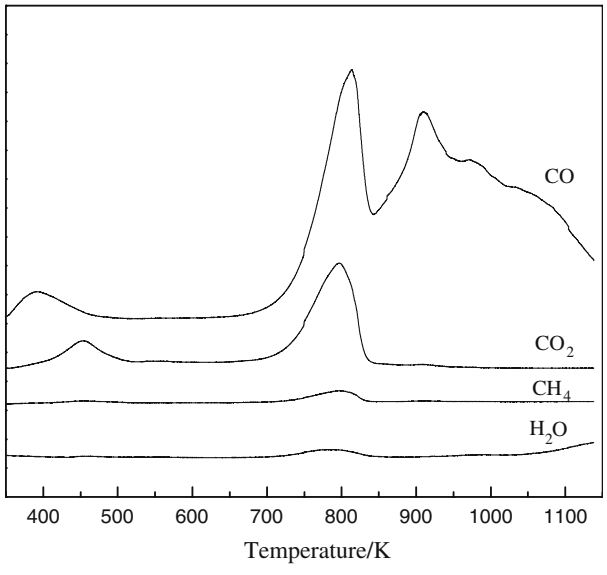

Figure 4. CO-TPD spectra of Co /AC catalyst.

As shown in figure 4, two CO_2 peaks are observed at 450 and 811 K. It is observed that the appearance of CO_2 is accompanied by the production of CH_4 and H_2O at 811 K during the desorption of chemisorbed CO. It is interesting that the CH_4 and H_2O desorption peaks are coincident with the CO_2 desorption peak. CO_2 can be produced during CO-TPD by the disproportionation of CO and the formation of CH_4 and H_2O can be explained in terms of the following reaction sequence: $CO + S \rightarrow CO_s$ (1), $CO_s + S \rightarrow C_s + O_s$ (2), $CO + O_s \rightarrow CO_2 + S$ (3) [29], $C_s + H_s \rightarrow CH_4$ (4), $O_s + H_s \rightarrow H_2O$ (5). We noted that there was a lack of H_2 formation in CO adsorption–desorption experiments. The explanation for active hydrogen can probably be ascribed to the decomposition of surface groups on the support surface. Another possible reason suggested that hydrogen comes from the reduction process of catalyst. Active hydrogen cannot be completely removed during reduction unless by heating to high temperatures at which sintering occurs. The CH_4 comes from interaction of active hydrogen with surface-active carbon species followed by the formation during CO dissociation. At the same time, the observed production of H_2O during CO-TPD indicates that H_2O is formed by the reaction of the hydrogen atom with surface-active oxygen species.

Figure 5 shows the effect of vanadium loadings on the amount of desorption of adsorbed CO in the CO-TPD experiment. Tejuca *et al.* [30] reported that the low temperature peak of the TPD profiles of the oxidized $LaCoO_3$ assigned to desorption of adsorbed CO on Co^{2+} sites and the high temperature peak assigned to CO species on metallic Co sites. When vanadium promoter is added, the amount of CO desorption at 811 K enhances while the amount of a weakly adsorbed CO at 392 K decreases with increase of the vanadium addition. Obviously, it demonstrates that an addition of V can favor to enhance the strongly adsorbed CO as well as decrease the weakly adsorbed CO.

The effect of V loading on the amounts of the formation of CO_2, CH_4 and H_2O during CO-TPD is also shown in figure 5. The relative intensity of CO_2, CH_4 and H_2O of V–Co/AC catalysts increases with the V loading. These results indicate that the presence of V in the Co/AC catalyst promotes the dissociation of the C–O bond.

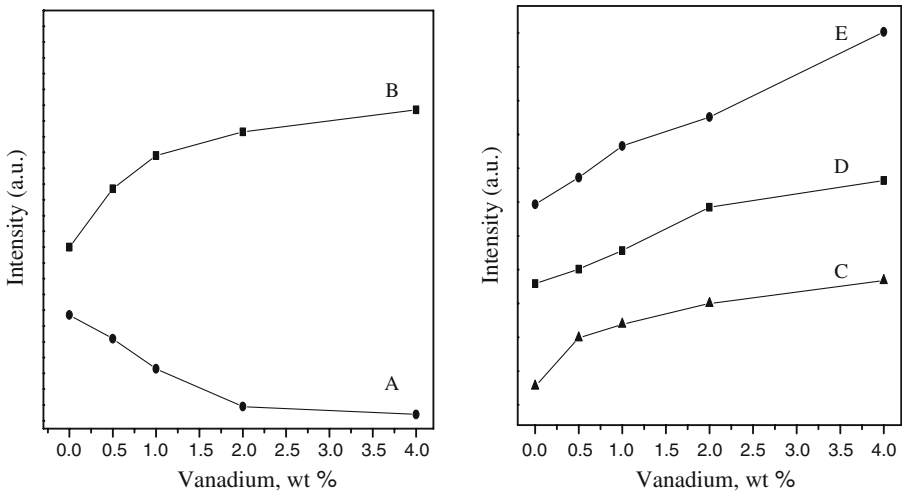

Figure 5. Intensities of desorption species versus vanadium loadings of V–Co/AC catalysts (a) CO desorption at 392 K; (b) CO desorption at 811 K; (c) CO_2 desorption; (d) CH_4 desorption; (e) H_2O desorption.

3.4. Temperature-programmed surface reaction (H_2-TPSR)

The reactivity of chemisorbed CO under H_2 flow can provide useful information about the ability of V species to dissociate and hydrogenate CO molecule, since the hydrogenation of surface-active carbon species into methane is very fast on the catalyst surface, methane formation can be used as a tool for measuring the CO dissociation and hydrogenation [31].

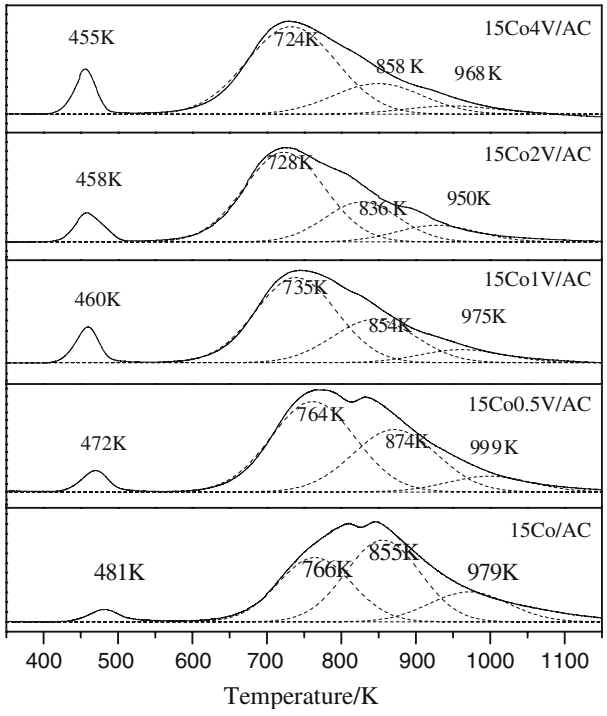

Figure 6. Methane peak during H_2-TPSR of adsorbed CO over V-promoted Co/AC catalysts.

Figure 6 displays the H_2-TPSR spectra of adsorbed CO on Co/AC and V–Co/AC catalysts. There are four methane peaks in H_2-TPSR spectra of the Co/AC catalyst. The former two CH_4 peaks at 481 K and 766 K suggest the formation of two types of carbon species from the chemisorbed CO. The other two peaks are assigned to the interaction of hydrogen with the different surface oxygen-containing groups on the activated carbon surface at 855 K and 979 K. The desorption temperature of the first CH_4 peak is close to the reaction temperature of F-T synthesis, while the desorption temperature of the other CH_4 peaks are higher than the reaction temperature of the F-T reaction. Four peaks of methane formation are also observed in the H_2-TPSR spectra over the V–Co/AC catalysts. The first peak is shifted from 481 K to 472 K, 460 K, 458 K and 455 K when V loadings increase from 0 to 0.5, 1, 2 and 4 wt.%, respectively, indicating that the addition of V facilitate metallic cobalt to dissociate the CO molecules and increase the concentration of surface-active carbon species. Moreover, the relative intensity of methane for V–Co/AC increases with V loading increasing. The above observation further confirms that the presence of vanadium favors to enhance the ability of CO dissociation and increase reaction activity of the CO hydrogenation.

3.5. Fischer–Tropsch synthesis

The catalyst activity and product distribution of the catalysts with various V loadings are shown in table 3. CO conversion increases unexpectedly from 38.9% to 87.4% when 4 wt.% V is doped into Co/AC samples. The CH_4 selectivity decreases from 20.4% to 12.1% when 0.5 wt. % V is added into the Co/AC catalyst, while C_5^+ selectivity increases from 61.4 to 72.0 %. But, excess of vanadium can increase methane selectivity and decrease C_5^+ selectivity.

Table 3
The effect of V loading on the activity and selectivity of Co/AC catalysts

Catalyst	CO conv. (%)	Hydrocarbon distribution (wt.%)						ASF (α)
		C_1	C_{2-4}	C_5–C_9	C_{10}–C_{20}	C_{21}^+	C_5^+	
15Co	38.9	20.4	18.2	30.9	28.8	1.7	61.4	0.75
15Co0.5V	45.3	12.1	15.9	34.3	35.3	2.4	72.0	0.83
15Co1V	56.5	13.9	17.5	34.2	32.2	2.2	68.6	0.82
15Co2V	73.1	15.3	18.8	29.9	34.3	1.7	65.9	0.81
15Co4V	87.4	18.4	18.7	28.1	33.5	1.3	62.9	0.76

Conditions: $T = 493$ K, $P = 2.5$ Mpa, GHSV = 500 h^{-1}, $H_2/CO = 2$.

4. Conclusions

Small amount of V addition into Co/AC catalysts remarkably exhibits low methane selectivity and high selectivity toward middle distillates, but excess V addition can decrease C_5^+ selectivity and increase methane selectivity. CO-TPD and H_2-TPSR results of adsorbed CO show that the existence of V significantly enhances C–O bond dissociation and favors the hydrogenation of surface-active carbon species.

Acknowledgments

The authors gratefully acknowledged the financially support from BP-CAS Project of Clean Energy facing the future.

References

[1] R.B. Anderson, *The Fischer–Tropsch synthesis* (Academic Press, New York, 1984).
[2] S.L. Sun, N. Tsubaki and K. Fujimoto, Appl. Catal. A 202 (2000) 121.
[3] Z.R. Li, Y.L. Fu, M. Jiang, T.D. Hu, T. Liu and Y.N. Xie, J. Catal. 199 (2001) 155.
[4] F. Rodríguez-Reinoso and A. Sepúlveda-Escribano, Appl. Catal. A 77 (1991) 95.
[5] D. Schanke, S. Vada, E.A. Blekkan, A.M. Hilmen, A. Hoff and A. Holmen, J. Catal. 156 (1995) 85.
[6] E. Iglesia, Appl. Catal. A 161 (1997) 59.
[7] A. Kogelbauer, J.G. Goodwin Jr. and R.J. Oukaci, J. Catal. 160 (1996) 125.
[8] C.H. Mauldin, US Patent 4568663 (1986).
[9] J.S. Ledford, M. Houalla, A. Proctor and D.M. Hercules, J. Phys. Chem. 93 (1989) 6770.
[10] J. Barrault, A. Guilleminot, J.C. Achard, V. Paul-Boncour and A. Percheron-Guegan, Appl. Catal. A 21 (1986) 307.
[11] S. Ali, B. Chen and J.G. Goodwin Jr., J. Catal. 157 (1995) 35.
[12] F. Rohr, O.A. Lindvåg, A. Holmen and E.A. Blekkan, Catal. Today 58 (2000) 247.
[13] H. Beuther, C.L. Kibby, T.P. Kobylinski and R.B. Pannell, US Patent 4717702 (1988).
[14] G.V.D. Lee and V. Ponec, Catal. Rev. 29 (1987) 183.
[15] S. Eri and J.G. Goodwin Jr., US Patent 4857559 (1989).
[16] A. Guerrero-Ruiz, A. Sepúlveda-Escribano and I. Rodríguez-Ramos, Appl. Catal. A 120 (1994) 71.
[17] W.P. Ma, Y.J. Ding and L.W. Lin, Ind. Eng. Chem. Res. 43 (2004) 2391.
[18] T. Wang, Y.J. Ding, J.M. Xiong, W.M. Chen, Z.D. Pan, Y. Lu and L.W. Lin, Stud. Surf. Sci. Catal. 147 (2004) 349.
[19] B. Ernst, L. Hilaire and A. Kiennemann, Catal.Today 50 (1999) 413.
[20] A.Y. Khodakov, J. Lynch, D. Bazin, B. Rebours, N. Zanier, B. Moisson and P. Chaumette, J. Catal. 168 (1997) 16.
[21] P. Arnoldy and J.A. Moulijn, J. Catal. 93 (1985) 38.
[22] B. Viswanathan and R. Gopalakrishnan, J. Catal. 99 (1986) 342.
[23] R.D. Oades, S.R. Morris and R.B. Moyes, Catal. Today 7 (1990) 199.
[24] C.L. Bianchi, Catal. Lett. 76 (2001) 155.
[25] J.L. Li, G. Jacobs, Y.Q. Zhang, T. Das and B.H. Davis, Appl. Catal. A 223 (2002) 195.
[26] J. Cortes and S. Droguett, J. Catal. 38 (1975) 477.
[27] I. Rodríguez-Ramos, A. Guerrero-Ruiz and J.L.G. Fierro, Appl. Surf. Sci. 40 (1989) 239.
[28] S. Haydar, C. Moreno-Castilla, A. Ferro-García M., F. Carrasco-Marín, J. Rivera-Utrilla, A. Perrard and J.P. Joly, Carbon 38 (2000) 1297.
[29] G.G. Low and A.T. Bell, J. Catal. 57 (1979) 397.
[30] L.G. Tejuca, A.T. Bell, J.L.G. Fierro and M.A. Peña, Appl. Surf. Sci. 31 (1988) 301.
[31] K. Fujimoto, M. Kameyama and T. Kunugi, J. Catal. 61 (1980) 7.